JOURNAL OF AIRCRAFT
Vol. 46, No. 4, July–August 2009

Engineering Notes

Bubble Burst Control for Stall Suppression on a NACA $63_1 - 012$ Airfoil

C. W. Wong* and K. Rinoie†
University of Tokyo, Tokyo 113-8656, Japan

DOI: 10.2514/1.43924

Introduction

AFTER the laminar boundary layer separates from the airfoil surface, the flow can reattach to the surface as a turbulent shear layer. The region between the laminar separation and the reattachment is called a laminar separation bubble [1]. Depending on the chordwise extent of the laminar separation bubble, it can be classified as a short or long bubble. Once the short bubble fails to reattach to the airfoil surface, which is commonly known as a short bubble burst, the airfoil stalls abruptly. Some classical devices such as transition ramps [2], boundary-layer trips [3], and pneumatic turbulators [4] were developed to produce disturbances that could lead to the early flow transition of the boundary layer and consequently delay airfoil stall. Note that the technique of employing the boundary-layer trip strip on sail plane is still commonly used due to its simplicity and high effectiveness for a wide range of Reynolds numbers. The initial study of the control of the short bubble burst as a means to avoid airfoil stall was conducted by Rinoie et al. [5]. The novel concepts considered the use of a thin plate placed inside the short bubble to control the separated shear layer development artificially. Their experimental results revealed that the vortical structures originating from Kelvin–Helmholtz instabilities inside the separated shear layer are enhanced by those formed at the trailing edge of the plate, and this forces the separated shear layer to reattach downstream of the plate. As a result, both the stall angle and the maximum lift coefficient of the NACA 0012 airfoil section were increased. Kurita et al. [6] showed that the application of the rectangular plate was more effective compared with the thin plate that was applied onto the same airfoil section and that the leading-edge stall was further suppressed. Likewise, the circulated flow reattaches onto the airfoil surface and alters the lift characteristics near stall. However, the effectiveness of the plates was only demonstrated through the comparison of the lift characteristics of the airfoil, which were calculated from the pressure distributions. Both the drag force and the overall performance of the airfoil with the plate attachment were not investigated. Unless specified otherwise, these two types of plates are called "burst control plates." Note that this technology (the burst control plate) can be extensively used on low-speed unmanned aerial vehicles. An adverse effect of this technology arises from the existence of the plate at the front portion of the airfoil. The objectives of the present study are to expand the existing experimental data base and to extend the understanding of the effects of the application of the burst control plate on the aerodynamics characteristics.

Presented as Paper 1111 at the 47th AIAA Aerospace Sciences Meeting, Orlando, FL, 5–8 January 2009; received 19 February 2009; revision received 16 April 2009; accepted for publication 17 May 2009.

*Japan Society for the Promotion of Science Postdoctoral Fellow, Department of Aeronautics and Astronautics, School of Engineering, 7-3-1 Hongo, Bunkyo-ku. Member AIAA.

†Professor, Department of Aeronautics and Astronautics, School of Engineering, 7-3-1 Hongo, Bunkyo-ku. Senior Member AIAA.

Experimental Setup

Measurements were conducted in a subsonic suction-type wind tunnel with a freestream turbulent intensity of 0.16% at a freestream velocity of 10 m/s. A NACA $63_1 - 012$ airfoil with span of 200 mm and a chord length of 200 mm was employed. The Reynolds number based on the chord length is 1.3×10^5. The 12% thick section was selected for use in the present investigation because of the already existing data for this airfoil section (see [7]). The control of the short bubble burst was realized by attaching the burst control plate across the span and at the front portion of the airfoil. Two types of plates were used, the thin plate and the rectangular plate, which were demonstrated in [5,6], respectively. Both types of plates have a constant width along the span direction. The thickness and chordwise length of the thin plate are 0.3 and 10 mm, respectively. With the leading edge of the thin plate ($x/c = 0.025$, where c is the chord length of the airfoil and x is the Cartesian coordinate with the origin at the leading edge of the airfoil) fixed on the airfoil surface, the plate is tilted and the loose edge is 1 mm above the airfoil surface. On the other hand, the height and the chordwise length of the rectangular plate are 1 and 3.2 mm, respectively. For the rectangular plate, two positions (defined at the leading edge of the plate) were tested: $x/c = 0.034$ and 0.059. The layout of the thin plate and the rectangular plate are illustrated in Figs. 1a and 1b, respectively. Smoke flow visualization at the center of the airfoil span was conducted. An oil mist of Ondina oil was used as the flow visualization particles. A 500 W halogen lamp was used as a light source (the width of the light sheet was approximately 5 mm). The visualized flow was recorded using a digital camera. Aerodynamic forces were measured by a three-component external load cell connected to a 12-bit data acquisition system with a sampling rate of 512 Hz. The accuracy of the force measurement is approximately ±1%. Aerodynamic forces were normalized by the freestream dynamic pressure and airfoil area. Wind-tunnel wall corrections were made based on [8]. The initial tests were conducted on the baseline airfoil (without the plate attachment), and the results were compared with the airfoil with the burst control plate attachment.

Experimental Results

Smoke Flow Visualization

Figure 2 shows the flow patterns around the airfoil (with and without the plate attachment) at the stall angle. Note that these stall angles were determined by the force measurements, where the lift coefficient C_1 denotes the maximum (except in Figs. 2a and 2b) and the physical parameters of the burst control plate including the height h and the width w were normalized by the airfoil chord c.

Figure 2a shows that the laminar flow separation occurs in the vicinity of the leading edge of the baseline airfoil at $\alpha = 9.5$ deg and that the separated flow reattaches on the airfoil surface as turbulent flow at a location very close to the leading edge. The short bubble is formed between the separation location and the reattachment location. Figure 2b indicates the flow patterns around the baseline airfoil after stall (at $\alpha = 10.5$ deg). It clearly shows that the separated laminar flow in the vicinity of the leading edge of the airfoil fails to reattach to the surface (i.e., short bubble burst) and that a reversed flow is established. The result of this reversed flow phenomenon is to create a large wake of recirculating flow downstream of the surface. Note that the airfoil stalling characteristics depend on

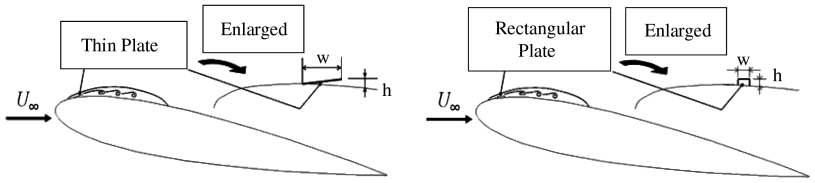

a) Thin plate **b) Rectangular plate**

Fig. 1 Illustration of the burst control plates [5,6].

both the turbulent boundary-layer separation at the rear portion of the airfoil, which moves upstream with an increasing angle of attack, and the occurrence of the short bubble burst at the front portion of the airfoil.

Figure 2c shows that the thin plate is attached to the airfoil at $\alpha = 10.5$ deg and that the flow structure including the short bubble formation near the leading edge of the airfoil is similar to the one in Fig. 2a. Even though the angle of attack in Fig. 2c is set higher than the one in Fig. 2a, the large flow separation is avoided. This is mainly due to the fact that the strength of the vortical structures inside the separation bubble is enhanced by the trailing edge of the thin plate. This clearly demonstrates the benefit of the thin plate as the airfoil stall is suppressed. Figure 2d shows that the rectangular plate is attached to the airfoil at $\alpha = 12$ deg. At this high angle of attack, the attached flow occurs over the front portion of the airfoil, which is remarkable, although the flow separates again at about $x/c = 0.5$. This clearly demonstrates the effectiveness of the rectangular plate. The result suggests that the momentum of the reattached turbulent flow, which affected by the rectangular plate (in case 3, as shown in Fig. 2d), is much lower than the thin plate in case 2 (as shown in Fig. 2c). As a result, the pressure drag in case 3 at $\alpha = 12$ deg (mainly due to the increase of the chordwise extent of the turbulent boundary-layer separation at the rear portion of the airfoil) is higher than the value in case 2 at the stall angle ($\alpha = 10.5$ deg) as seen in the force measurements.

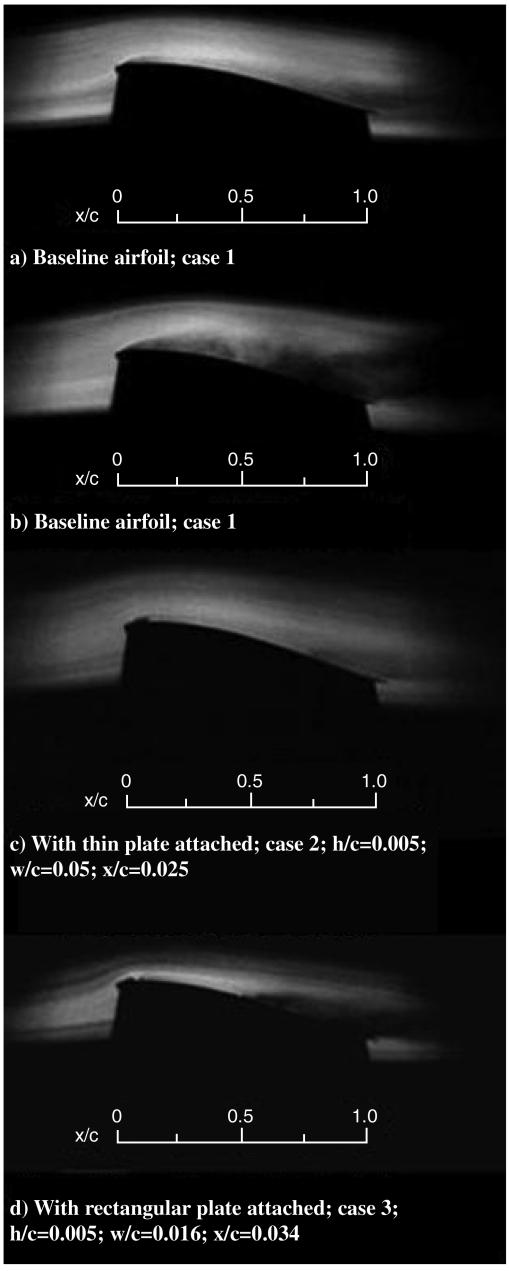

Fig. 2 Smoke flow visualization for different cases: a) $\alpha = 9.5$ deg, b) $\alpha = 10.5$ deg, c) $\alpha = 10.5$ deg, and d) $\alpha = 12$ deg.

Force Measurements

Figure 3 shows the lift coefficient C_l for cases 1, 2, 3, and 4. (Note that the configuration of each case, except case 4, is labeled in Fig. 2; case 4 mainly demonstrates the effect of displacing the rectangular plate downstream.) Because of the uncertainty of less than 0.1 deg for the angle of attack α, the lift coefficient of the baseline airfoil at $\alpha = 0$ deg does not equal zero and this error is consistent for all cases. When the burst control plate is attached to the airfoil surface and α is less than 9 deg, the lift coefficient is reduced compared with the value of the baseline airfoil. Note that the short bubble at $\alpha \leq 5$ deg does not occur at the front portion of the NACA 63_1-012 airfoil section, as discovered in [7]. The laminar flow in the vicinity of the leading edge of the airfoil is artificially tripped, which produces a boundary-layer transition region and reduces the suction pressure. The reduction in the lift coefficient is reduced when α is greater than 5 deg, because the burst control plate is actually located within the short bubble. It becomes obvious that the use of the burst control plate at any angle of attack less than 9 deg is detrimental to the flowfield on the suction surface of the airfoil.

When α is between 9 and 12 deg, the lift coefficient for cases 2, 3, and 4 is significantly higher than the value of the baseline airfoil. In particular, the lift coefficient at $\alpha = 11.2$ in case 3 is 0.985, which is over 17% higher than the value of the baseline airfoil. The turbulent boundary-layer separation moves gradually from the trailing edge of the airfoil with increasing angle of attack. Herein, the trailing-edge stalling only occurs if the flow separation starting from the trailing edge of the airfoil is observed when stall occurs. When the lift

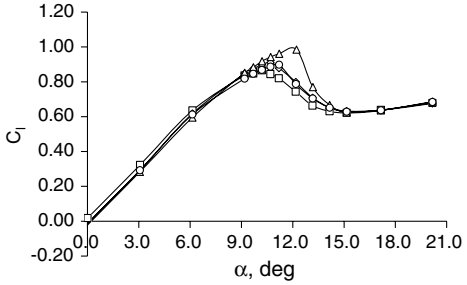

Fig. 3 Comparisons of lift coefficient: □, case 1 (baseline airfoil); ◇, case 2 ($h/c = 0.005$, $w/c = 0.05$, $x/c = 0.025$); △, case 3 ($h/c = 0.005$, $w/c = 0.016$, $x/c = 0.034$); and ○, case 4 ($h/c = 0.005$, $w/c = 0.016$, $x/c = 0.059$).

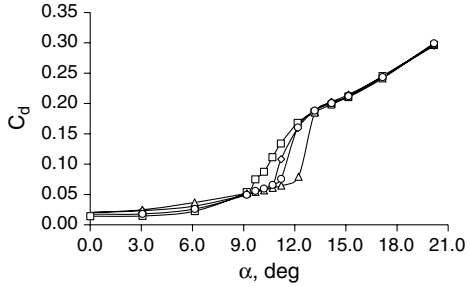

Fig. 4 Comparisons of drag coefficient: □, case 1 (baseline airfoil); ◇, case 2 ($h/c = 0.005$, $w/c = 0.05$, $x/c = 0.025$); △, case 3 ($h/c = 0.005$, $w/c = 0.016$, $x/c = 0.034$); and ○, case 4 ($h/c = 0.005$, $w/c = 0.016$, $x/c = 0.059$).

coefficient for case 2 is compared with value for case 4 (note that the trailing-edge location and the height of both plates in these two cases are the same), it can be seen that these two lift curves are almost overlapping with each other. The lift coefficient for case 2 is slightly higher than the value for case 4 when α is between 9 and 12 deg. The reduction of C_1 is mainly due to the difference in the geometry of the plate, which affects the formation of the vortical structures generated by the plates.

As the short bubble moves forward along the airfoil surface with increasing angle of attack, it is subjected to an increase in the local velocity, which reduces its chordwise extent. However, the increased curvature of the airfoil surface in the vicinity of the leading edge makes it more difficult for the separated flow to reattach to the surface and this condition becomes rather obvious when α is higher than 12 deg. Therefore, when the effect of the curvature overcomes the effect of the increased velocity, the flow does not reattach to the airfoil surface and the amount of lift that is lost (above the stall angle) depends on the extent of the turbulent flow separation over the entire portion of the airfoil.

Figure 4 compares the drag coefficient C_d for cases 1, 2, 3, and 4. At $\alpha = 0$ deg, the drag coefficient for cases 2, 3, and 4 is slightly higher than the value for case 1 (baseline airfoil). Because of the presence of the burst control plate at the front portion of the airfoil, the boundary-layer transition region (originating aft of the plate) extends in the chordwise direction. The burst control plate acts like a boundary-layer trip strip at α between 0 and 3 deg. The drag increase in cases 2, 3, and 4 comes from the skin friction due to the transition region that exists over the suction surface of the airfoil. The drag at α between 3 and 6 deg in cases 2, 3, and 4 is significantly higher than the value for the baseline airfoil because of the small separation–reattachment region that exists at the leading edge of the airfoil. The burst control plate on the surface of the airfoil increases the surface roughness in the flowfield near the leading edge of the airfoil. When the sharp leading edge of the rectangular plate is positioned at its most forward location (i.e., in case 3), the extent of the separation–reattachment region is deemed to be large.

In contrast, the drag is successfully suppressed when the burst control plate is applied to the airfoil at α between 9 and 11.2 deg. In particular, the drag coefficient for case 3 is significantly lower than the values for the other cases (cases 1, 2, and 4). Because the chordwise length of the short bubble is reduced when the burst control plate is attached to the airfoil surface, as shown in smoke flow visualization, the drag coefficient mainly depends on the extent of the turbulent boundary-layer separation over the rear portion of the airfoil. Note that the maximum drag reduction is over 100% when case 3 is compared with case 1 and that the performance of the airfoil (L/D ratio) is greatly increased between these angles of attack. On the other hand, the drag coefficient increases gradually due to the turbulent boundary-layer separation at the rear portion of the airfoil moving upstream with increasing angle of attack. When α is above 13 deg, the drag coefficient of all cases are approximately identical.

Conclusions

The novel concept of the burst control plate was investigated on a NACA $63_1 - 012$ airfoil section at a chord Reynolds number of 1.3×10^5. The lift coefficient for the airfoil with the burst control plate attachment is significantly higher than the value for the baseline airfoil at α between 9 and 12 deg. In particular, the lift coefficient of case 3 at $\alpha = 11.2$ deg is 0.985, which is over 17% higher than the value of the baseline airfoil. The stall angle of the airfoil with the burst control plate attachment was postponed. The drag of the airfoil with the burst control plate attachment at α between 9 and 12 deg is greatly reduced. The short bubble burst is effectively suppressed, and the drag of the airfoil mainly depends on the extent of the turbulent boundary-layer separation over the rear portion of the airfoil. The application of the burst control plate on the NACA $63_1 - 012$ airfoil section is effective in terms of stall suppression. However, the use of the burst control plate at any angle of attack less than 9 deg is detrimental to the flowfield on the suction surface of the airfoil. Ongoing research using particle image velocimetry measurements aims to reveal the flow interactions (including the flow turbulent intensity) at and aft of the location of turbulent flow reattachment. Hence, this could identify the reasons for the detrimental effect on performance at low angles of attack, and implementation of these burst control plates could be anticipated.

Acknowledgments

The research was supported by the Japan Society for the Promotion of Science. A special thanks to Satoshi Kurita and Yasuto Sunada for their beneficial help in all experimental work.

References

[1] Tani, I., *Low-Speed Flows Involving Bubble Separation*, Progress in Aeronautical Sciences, Vol. 5, Pergamon, New York, 1964, pp. 70–103.

[2] Eppler, R., and Somers, D. M., "Airfoil Design for Reynolds Numbers Between 50,000 and 500,000," *Proceedings of Low Reynolds Number Airfoil Aerodynamics Conference*, University of Notre Dame, Notre Dame, IN, 1985, pp. 1–14.

[3] Van Ingen, J. L., and Boermans, L. M. M., "Aerodynamics at Low Reynolds Numbers: A Review of Theoretical and Experimental Research at Delft University of Technology," *Proceedings of Aerodynamics at Low Reynolds Numbers Conference*, Vol. 1, Royal Aeronautical Society, London, 1986, pp. 1.1–1.40.

[4] Pfenninger, W., and Vemuru, C. S., "Design of Low Reynolds Number Airfoils," *Journal of Aircraft*, Vol. 27, No. 3, 1990, pp. 204–210. doi:10.2514/3.45920

[5] Rinoie, K., Okuno, M., and Sunada, Y., "Airfoil Stall Suppression by Use of a Bubble Burst Control Plate," *AIAA Journal*, Vol. 47, No. 2, 2009, pp. 322–330. doi:10.2514/1.37352

[6] Kurita, S., Rinoie, K., and Sunada, Y., "Stall Suppression by Use of a Rectangular Cross Section Plate Placed on NACA0012 Airfoil," *Proceedings of the 40th Fluid Dynamics Conference*, Japan Society for Aeronautical and Space Sciences, Tokyo, June 2008, pp. 331–334.

[7] Rinoie, K., Ichikawa, K., and Sunada, Y., "Behavior of Laminar Separation Bubble Formed on NACA 631-012," *Journal of the Japan Society for Aeronautical and Space Sciences*, Vol. 51, No. 597, 2003, pp. 582–584. doi:10.2322/jjsass.51.582

[8] Allen, H. J., and Vincenti, W. G., "Wall Interference in a Two-Dimensional-Flow Wind Tunnel, with Consideration of Compressibility," NACA Rept. 782, 1944.